Determination of the impact of strain rate on dynamic recrystallization of hot-deformed 2205 duplex stainless steel

A. D. Baruwa*[a], E. Gonya[a] and M. E. Makhatha*[a]

[a]Department of Metallurgy, University of Johannesburg, South Africa

Corresponding Author(s): emakhatha@uj.ac.za; darebaruwa@gmail.com

Abstract

2205 duplex stainless steel suffers poor hot workability, especially whe1981hot-deformed. This investigation aims to determine the strain rate's effect on the material's dynamic recrystallization after heat treatment. Secondly, to ascertain the critical strain at which the recrystallization occurs. The as-rolled material was subjected to heat treatment at 1340 °C for some time. After heat treatment, the yielded equiaxed austenite morphology was used for this investigation. Gleeble 1500™ thermo-mechanical was used as a simulant in uniaxial compression mode. The deformation temperature was set at 850 °C, with maximum strain at 0.8 and carried out at 0.001 s^{-1}, 0.01 s^{-1}, 0.1 s^{-1}, 1 s^{-1}, 5 s^{-1} strain rates. The microstructure of before and after heat-treatment was evaluated using a light microscope, while the critical factors (stress and strain) were determined through the stress-strain curve. It was observed that the lowest strain rate generated the maximum critical stress and critical strain at 191.99 MPa and 0.08283, respectively. However, at the highest strain rate, the maximum critical stress and critical strain experienced by the material were at 336.32 MPa and 0.17577. Overall, it was established that the applied stain rate influenced the critical strain and stress of the material. It can be concluded that dynamic recrystallization can occur at any strain rate, but the applied stress determines the extent of the phenomenon.

Keywords: Critical Strain; Critical Stress; Dynamic Recrystallization; Morphology; Stress-Strain

1. Introduction

Due to a higher susceptibility of austenitic stainless steels (ASSs) in aggressive environments and the price volatility of Nickel (Ni) in the international market year in-year out, have raised a cause for alternative stainless steels, among them duplex stainless steel (DSS). 2205 duplex stainless steel (DSS) is associated with dual phase- nearly equivalent austenite and ferrite phases. Its excellent mechanical properties (tensile strength and hardness), weldability and strong corrosion resistance have made the material one of the most sought [1–5]. Its applications spread over various sectors such as oil and gas, nuclear, petrochemical and marine, to mention a few [6,7]. However, its poor workability has limited its application at extremely high temperatures by causing stress corrosion cracking [8]. Production into smaller units, dimensions and shapes requires different fabrication methods and impacts the microstructure [9] and, therefore, influences the change in properties of the material [10]. This problem emerged from the disparity in compositions and properties of ferrite and austenite phases. The ferrite phase is soft with high stacking fault energy and low thermal strength, which could result in clumping when subjected to hot deformation. On the other hand, austenite possesses hard characteristics with high thermal strength and low stacking fault energy that yields a suppressed dynamic recovery of dislocated gains during hot deformation [11].

During hot deformation, dynamic recrystallization (DRX) occurs and results in the refinement of the grains of a metallic material [12,13]. The refinement defines such material's microstructure and yielding properties [14]. Factors such as starting grain size, material's chemical properties, stacking fault energy, deformation strain and stress, temperature and thermo-mechanical properties influence the behaviour of a material undergoing DRX [15,16]. DRX is essential during hot deformation because it helps to determine the flow stress material experiences at a steady state. DRX can be continuous (increment in the misoriented grains) or discontinuous (protuberance of existing grains) [17]. The occurrence of DRX as a result of the thermal deformation process has established that the evolution of twin density and grain growth occurred due to recrystallization [18].

This activity affects the grain boundaries by causing many changes in the kinetics, such as grain boundary profile, grain boundary position, grain boundary composition, grain boundary structure and shear across the grain boundaries, among others [19]. On these effects, grain boundaries are classified as low-angle grain boundaries (LAGB) and high-angle grain boundaries (HAGB) based on misorientations of nucleated grains lattice [20] and grain boundary plane orientation [21,22]. Hu et al. [23] investigated the impact of grain boundary on the plasticity and ductility of the

polycrystalline metal and discovered that increase in gain boundary density could increase the back stress and reduce the ductility of a polycrystalline material.

True stress-strain flow curve, work hardening rate vs true stress [15], including microstructural evolutions [24], are often used to determine the critical stress and strain. Critical strain can be described as the minimum energy required to initiate dynamic recrystallization of a material. It is a factor used in predicting the softening mechanism during the deformation process [14]. This prediction can be made by physical evaluation (microstructural) or calculation (analytical and constitutive models). Previous research has deeply studied critical strain, critical stress and peak stress of the as-rolled hot- or cold-deformed 2205 DSS [11]. From the previous investigation, it was established that DRX thermal deformation parameters such as temperature, strain rate, and strain influence the nucleation of twin grains. These parameters also define the kinetic process and relationship between the thermal deformation process and conditions can be predicted by adopting flow stress Equations 1-3 as described by Mandal *et al.* [25]. Equation 1is a power function that is used at lower stress, while Equation 2 is an exponential function for moderate stress values. However, Equation 3 is a hyperbolic sine function that is applicable to all kinds of stress. Dynamic analysis of a material defines its kinetics in determining the constitutive equation to predict the flow stress at high temperatures.

$$\dot{\varepsilon} = A_1 \sigma^{n_1} exp\left(-Q/RT\right)(\alpha\sigma < 0.8) \qquad \text{Equation 1}$$

$$\dot{\varepsilon} = A_2 exp(\beta\sigma)\left(-Q/RT\right)(\alpha\sigma > 1.8) \qquad \text{Equation 2}$$

$$\dot{\varepsilon} = A[sinh(\alpha\sigma)]^n exp\left(-Q/RT\right)(for\ all\ stress) \qquad \text{Equation 3}$$

Where A_1, A_2, A, n_1, n, α, and β are constants associated with steel and $\alpha = \beta/n_1$. However, Q, T, α, $\dot{\varepsilon}$ and R represent thermal deformation activation energy (KJ/Mol), deformation temperature (K), peak stress (MPa), strain rate (s^{-1}) and molar gas constant (R=8.3145 J/(mol. K)), respectively.

In the past, detailed investigations on the thermochemical treatments, such as carburizing, surface mechanical attrition treatment (SMAT), nitriding, and heat treatment, were conducted on 2205 DSS to improve the material's microstructure and other properties and to further characterize for different applications. Most often, these treatments are conducted largely as surface modification. Carburizing was conducted on 2205 DSS to enhance the hardness and wear resistance by conducting salt-bath nitro-carburizing at low temperatures [26]. It is one of the methods that is being used to harden steel surfaces for improved strength and wear resistance. SMAT is a form of plastic deformation that was invented to cause grain refinement at the surface of a material to increase the yield strength, surface hardness, ultimate tensile strength and wear resistance. The process was applied to 2205 DSS, and a rise in the dislocation density was observed, also, the creation of a martensite phase in the region where SMAT was applied [27]. Nitriding is the process of modifying a surface by which nitrogen is combined with other alloying elements, such as iron. It has been used to alter the surface 2205 DSS at low temperatures to improve the material's wear resistance, surface hardness, fatigue life and stability in a chlorine-rich environment [28]. Chemical etching is the process by which a material's surface is oxidized by chemical or electrochemical, for example, hot nitric acid, in order to enrich and enhance the surface functionality and surface area, respectively. Dai et al. [29] subjected 2205 DSS to chemical etching and improved the corrosion resistance at a low temperature of 30 °C. Different types of heat treatments are available and have been applied to different materials, ranging from plastics, fibres, thermosets, glass, and metals, among others. Additive manufactured 2205 DSS was heat treated at 1000 ◦C for 10 minutes, it was observed that the microstructure reverted to the ferrite-austenite phase balance [30].

Before subjecting the material to the deformation process, there is limited or no detailed investigation into the heat-treated as-rolled 2205 DSS. Heat treatment has proven to be one of the methods to recrystallize and improve the microstructure of a material [31]. To improve tensile strength, TRIP-Aided Mo-Free Lean DSS was aged between 600 – 1000 °C for two hours after initial solution treatment at 1100 °C [32]. Aluminium type AA6061 and AA6063 heat-treated at T6-1 and T6-2 showed a change in the microstructural characteristics and improved mechanical strength of the materials [33]. It has been established that heat treatments do initiate dynamic recrystallization [34].

However, broad research has only been conducted on the critical strain and the effect of strain rate on the as-rolled 2205 DSS material. This investigation aims to determine the effect of strain rate on dynamic recrystallization that would aid in restricting the initiation of crack propagation of heat-treated deformed DSS 2205. This research would

assist in understanding forming and forging of materials and components, for example, high-pressure vessel parts such as anchors.

2. Materials and Methods

10 mm diameter rods of hot-rolled 2205 duplex stainless steel were locally sourced in the Republic of South Africa and cut into 15mm pieces for this investigation. The chemical composition of the material was determined using a spark spectrometer and wt. % generated was: 0.022 C, 0.480 Si, 1.181 Mn, 0.018 P, < 0.100 S, 22.350 Cr, 3.223 Mo, 5.557 Ni, 0.270 Cu, 0.033 Al, balance -Fe. The as-received materials were solution heat-treated in their rough state using an Elite™ tube furnace to achieve equiaxed microstructures, as presented in Figure 1.

10 samples (2 for each strain rate) were prepared for this investigation. A Gleeble 1500™ thermo-mechanical simulator was used for the compression. The effects of friction and barreling were eliminated by insetting Tantalum foils between the samples and anvils, as presented in Figure 2. The parameters for the experiment were set according to Table 1. The dynamic recrystallization was determined by plotting true stress vs true strain as well as work hardening rate vs applied stress. After an adequate metallography preparation of the material, Brunker™ optical emission spectrometer (Q4 TASMAN series 2) was used to investigate the microstructure of the material.
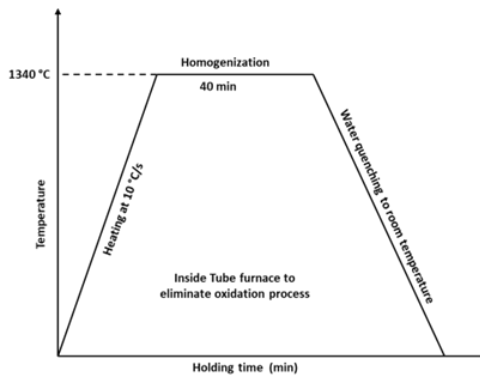

Figure 1: Description of the heat solution employed to achieve an equiaxed microstructure from as-rolled 2205 DSS
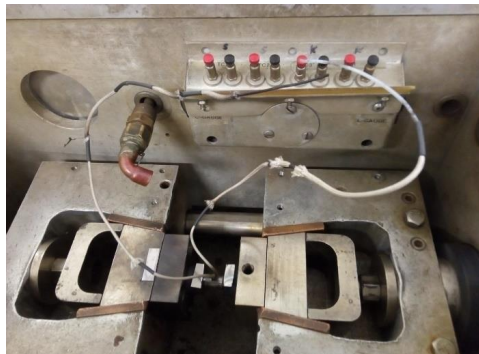

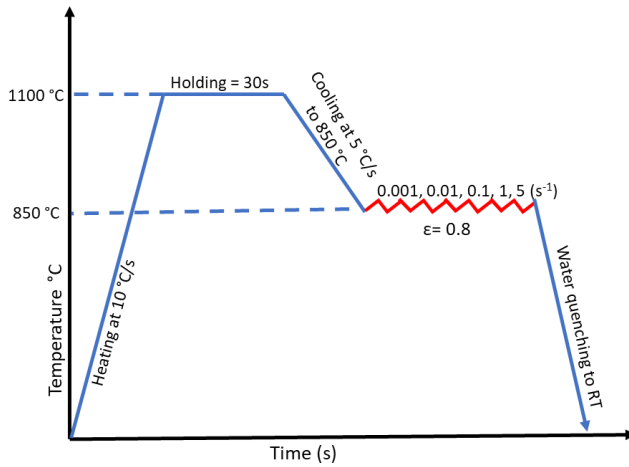Figure 2: Specimen arrangement in the Gleeble simulator

Figure 3: Gleeble hot deformation detailed process setup

Figure 3 represents the details of the isothermal uniaxial deformation of the working sample by compression. The sample was heated to a temperature of 1100 °C at the rate of 10 °C/s and held at that temperature for 30s for adequate homogenization. It is then cooled down to the deformation temperature of 850 °C at the rate of 5 °C/s in the furnace to allow for uniform diffusion and then compressed. The deformation was done at strain rates of 0.001 s^{-1}, 0.01 s^{-1}, 0.1 s^{-1}, 1 s^{-1}, 5 s^{-1} to reach the maximum set strain of 0.8. Thereafter, the deformed sample was quenched in water at room temperature in order for the specimens to retain their microstructures.

3. Results and Discussion

3.1 Microstructural analysis

Figure 4a indicates the as-rolled 2205 DSS, while 3b shows the equiaxed microstructure after the heat treatment of the as-rolled. Figure 3b establishes the redistribution and orientation of the microstructure after heat treatment. The dark grey indicates the ferrite (β) b phase and shows to be dominant in the structure, while the light grey is the austenite (σ) phase, as confirmed from the energy dispersive X-ray spectroscopy (not shown). The as-rolled showed a thinned microstructure by exhibiting grains that aligned orthogonally in the rolling direction. It can also be described as a triggered anisotropic-like banded microstructure [35].
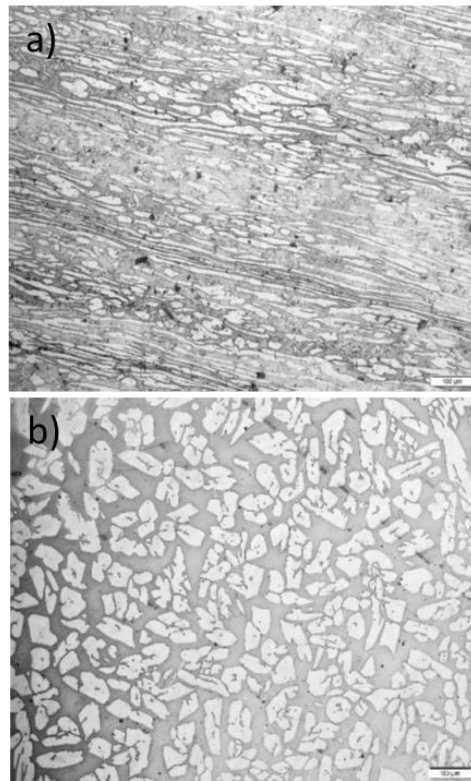
Figure 4: The yielded microstructure of a) as-rolled and b) equiaxed after solution treatment

Figure 4b displays almost equal fractions of phases of austenite and ferrite. The elongated structure of the as-rolled recrystallized to form a marginally elongated δ phase embedded in the coarse-grained γ phase matrix and appeared twinned. The sub-grain boundaries are more evident within the equiaxed matrix than in the as-rolled microstructure. The contrast observed in the microstructure can be attributed to the high strain of in-trapped ferrite accumulation. After the heat treatment, the fine and uniform microstructure exhibited by the working material will demonstrate good mechanical properties. It will also eliminate poor hot- workability associated with the material after rolling. Due to the yielded structure after heat treatment, the DRX can initiate at high temperatures and strain rates [36]. From the observation, the total density of non-defect grains increases compared to the number of defect grains after rolling, which is lowered by the grain boundary migration. In Figure 4b, discontinuous and continuous recrystallized grains are observed in the microstructure after the heat treatment. The mixed-type recrystallization phenomenon occurred because of new growth and nucleations of grains in the matrix. This will eliminate stress from the hot-rolling process and further reduce the residual stress trapped in the material. It can also be established that the mixed-type recrystallization will cause flow fluctuation in the stress-strain curve [37].

3.2 Hot deformation test

The deformation is carried out using Gleeble 1500^{TM,} and the results are plotted as a graph in terms of true stress vs true strain, representing the flow stress at a constant strain and temperature of 850 °C at the specified strain rates. The graph is plotted and presented in Figure 5a. A rise in flow stress is observed as the strain rate increases from 0.01 to 5 s-1. At the initial stage of the process, the flow stress increases sharply with an increase in the strain rate, which is initiated by the dislocations of grains and work hardening. It also establishes that work hardening happens until the peak stress is achieved and then decreases slowly without attaining the steady-state flow stress.
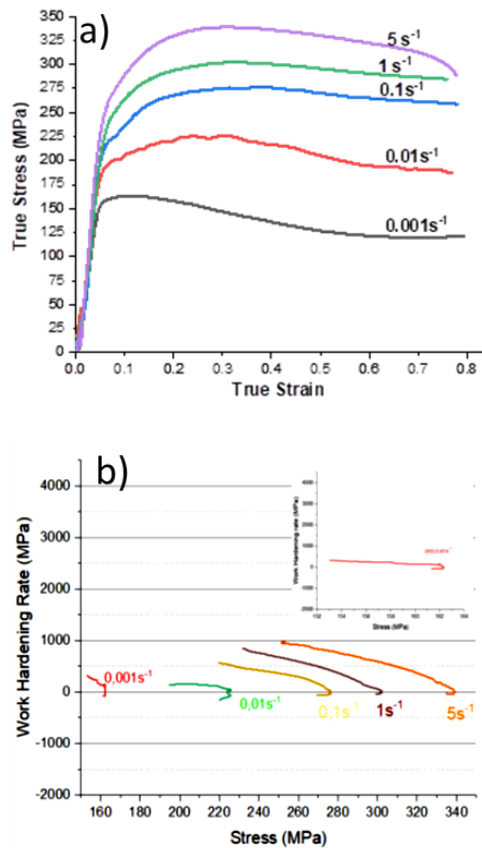
Figure 5: a) Stress-strain curve at different strain rates and b) the work hardening rate at different strain strains.

The flow stresses are impacted by the preset conditions for the deformation process. The higher the strain rate, the more the flow stress required increases [38]. Zener-Hollomon parameter fully describes the steady state behaviour of the material under deformation. Figure 5a shows two (0.001 s^{-1} and 0.01 s^{-1}) among the strain rates peak flow stress increase considerably due to work hardening and slowly decreases because of the dynamic softening emanating from dynamic recrystallization when the temperature of 850 °C is attained. In contrast, other strain rates maintain the same stress as the peak flow stress as a result of the dynamic recovery (DRV). This can be further explained as the residual balance between the hardening and softening mechanism. It also means that the dislocated grains' movement is hampered at higher strain rates. Therefore, the formation of unit cells or fusion of sub-grain boundaries would be challenging [39]. At higher strain rates, there will be shortening of thermal compression time and reduction in the ability of the activation energy to intitate recrystallization occurrence. The insufficient incubation time prevents recrystallization of the grains and further ineffectively able to terminate dislocation slips.

The extraction from the compression is presented in Table 1 below. Figure 5b is the work hardening rate vs applied stress graph at the stated strain rates, and it describes the inflection points between the yield stress and peak stress. As is evident, there are inflection points in all the strain rates and establishes the manifestation of dynamic recrystallization because the soft materials that undergo dynamic recovery do not show inflections.

Table 1: The extracted critical data from the plots

Strain Rate (s^{-1})	Critical Stress (MPa)	Critical Strain	Peak Stress (MPa)
0.001	161.99	0.08283	162.33
0.010	225.72	0.31448	226.00
0.100	276.07	0.30686	276.23
1.000	300.88	0.27501	302.35
5.000	336.32	0.17577	339.00

However, 0.01 s^{-1} displays double-inflection points, which translate to DRX and dynamic transformation (DT). DT is also a grain-refinement mechanism that requires a lower critical strain to get initiated [40] compared with DRX requirements. The relative graph of strain hardening rate vs true stress has been widely used to predict the critical stress of a material. This is transposed to the true stress vs true strain curve to deduce the critical strain that would initiate the DRX. At 0.001 s^{-1}, the values of the critical stress and strain are evaluated to be 161.99 MPa and 0.08283, respectively. However, the dynamic recrystallization of 5 s^{-1} is obtained at 336.32 MPa for critical stress and 0.17577 for critical strain. From Table 1, it can be concluded that a higher strain rate may not support the initiation of full DRX. It also means that when a higher strain rate is applied, there would be insufficient DRX to initiate softening effect in the sample [41]. From Table 1, the higher the strain rate, the lower the critical strain and the slower it would cause the initiation of DRX. This suggests that lower stress is required at a lower strain rate to start grain recrystallization and massive grain boundary migration at the substructures. It further establishes that minimal plastic deformation will occur at lower stress during grain migration, compared to significant stress required at higher strain rates- which could also generate plastic instability [22]. It has been established that plastic deformation is a definition of materials' evolution towards stationary and independent steady state [42]. At this state, there is a zero-strain hardening or softening rate, and it describes the peak stress and steady-state stress and their corresponding strains. The microstructure plays an important role in influencing the material's sensitivity to the strain rate. The phases and grain boundary arrangement (low-angle grain boundary and high-angle grain boundary) will define the work-hardening behaviour of the material at different strain rates [43]. The equiaxed microstructure here shows a large number of low-angle grains that will accommodate a high sensitivity to strain. In this case, the lower the strain rate, the finer the microstructure and the better the enhanced properties of the DSS 2205 [18]. This hot-deformation process will compact the ferrite grains, cause austenite grains to establish the DRX, and form twins at sub-grain boundaries.

4. Conclusion

This investigation examined the impact of strain rate on the DRX of the hot-deformed 2205 duplex stainless steel and the critical strain at which the process occurs. In other to improve the workability of the material after hot-rolling, the material was solution treated to initiate the initial recrystallization. The investigation fulfils the objectives, and the conclusions are as follows;

a) The strain rate has an effect on the material's grain recrystallization.

b) Also, it established that at a significant applied strain rate, the critical strain reduces as the applied stress increases.

c) The critical stress for the initiation of DRX is closer to the subjected peak stress on the material.

d) The softening mechanism is initiated at different strain values for each strain rate.

References

[1] O.E. Falodun, E.B. Mtsweni, S.R. Oke, P.A. Olubambi, Influence of Solution Heat Treatment on

Microstructure and Mechanical Properties of a Hot-Rolled 2205 Duplex Stainless Steel, J. Mater. Eng. Perform. 30 (2021) 7185–7194. https://doi.org/10.1007/s11665-021-05904-z.

[2]   Y. Zhao, C. Dong, Z. Jia, J. You, J. Tan, S. Miao, Y. Yi, Microstructure Characteristics and Corrosion Resistance of Friction Stir Welded 2205 Duplex Stainless Steel, Adv. Mater. Sci. Eng. 2021 (2021). https://doi.org/10.1155/2021/8890274.

[3]   J. Michalska, M. Sozańska, Qualitative and quantitative analysis of σ and χ phases in 2205 duplex stainless steel, Mater. Charact. 56 (2006) 355–362. https://doi.org/10.1016/j.matchar.2005.11.003.

[4]   S. Emami, T. Saeid, R.A. Khosroshahi, Microstructural evolution of friction stir welded SAF 2205 duplex stainless steel, J. Alloys Compd. 739 (2018) 678–689. https://doi.org/10.1016/j.jallcom.2017.12.310.

[5]   M. Yan, J. na Sun, H. gui Huang, L. Chen, K. Dong, Z. ye Chen, Effect of hot rolling and cooling process on microstructure and properties of 2205/Q235 clad plate, J. Iron Steel Res. Int. 25 (2018) 1113–1122. https://doi.org/10.1007/s42243-018-0172-6.

[6]   B. Varbai, T. Pickle, K. Májlinger, Effect of heat input and role of nitrogen on the phase evolution of 2205 duplex stainless steel weldment, Int. J. Press. Vessel. Pip. 176 (2019) 103952. https://doi.org/10.1016/J.IJPVP.2019.103952.

[7]   J. Yao, D.D. Macdonald, C. Dong, Passive film on 2205 duplex stainless steel studied by photo-electrochemistry and ARXPS methods, Corros. Sci. 146 (2019) 221–232. https://doi.org/10.1016/J.CORSCI.2018.10.020.

[8]   W. Shen, F. Wang, Z. Yang, C. Li, P. Lin, X. Zhu, Investigation of the Crack Initiation and Propagation in Super Duplex Stainless Steel During Hot Working, in: Miner. Met. Mater. Ser., Springer, 2020: pp. 157–167. https://doi.org/10.1007/978-3-030-36540-0_15.

[9]   S.R. Oke, O.O. Ige, O.E. Falodun, B.A. Obadele, M.B. Shongwe, P.A. Olubambi, Optimization of process parameters for spark plasma sintering of nano structured SAF 2205 composite, J. Mater. Res. Technol. 7 (2018) 126–134. https://doi.org/10.1016/J.JMRT.2017.03.004.

[10]   F.L. Dias, G. Cardeal Stumpf, S.S. Ferreira de Dafé, D.B. Santos, Homogenisation effect on mechanical and pitting behaviour of 2205 Duplex Stainless Steel, Mater. Sci. Technol. (United Kingdom). 36 (2020) 1796–1804. https://doi.org/10.1080/02670836.2020.1836738.

[11]   Y. Song, S. Wang, G. Zhao, Y. Li, L. Juan, Z. Jian, Hot deformation behavior and microstructural evolution of 2205 duplex stainless steel, Mater. Res. Express. 7 (2020) 46510. https://doi.org/10.1088/2053-1591/ab8529.

[12]   H.K. Zhang, H. Xiao, X.W. Fang, Q. Zhang, R.E. Logé, K. Huang, A critical assessment of experimental investigation of dynamic recrystallization of metallic materials, Mater. Des. 193 (2020) 108873. https://doi.org/10.1016/J.MATDES.2020.108873.

[13]   H. Pan, Y. He, X. Zhang, Interactions between dislocations and boundaries during deformation, Materials (Basel). 14 (2021) 1–48. https://doi.org/10.3390/ma14041012.

[14]   G. Varela-Castro, J.M. Cabrera, J.M. Prado, Critical strain for dynamic recrystallisation. The particular case of steels, Metals (Basel). 10 (2020) 135. https://doi.org/10.3390/met10010135.

[15]   Y. Li, Y. Zhang, Z. Chen, Z. Ji, H. Zhu, C. Sun, W. Dong, X. Li, Y. Sun, S. Yao, Hot deformation behavior and dynamic recrystallization of GH690 nickel-based superalloy, J. Alloys Compd. 847 (2020). https://doi.org/10.1016/j.jallcom.2020.156507.

[16]   K.K. Alaneme, E.A. Okotete, Recrystallization mechanisms and microstructure development in emerging metallic materials: A review, J. Sci. Adv. Mater. Devices. 4 (2019) 19–33. https://doi.org/10.1016/J.JSAMD.2018.12.007.

[17]   K. Huang, R.E. Logé, A review of dynamic recrystallization phenomena in metallic materials, Mater. Des. 111 (2016) 548–574. https://doi.org/10.1016/j.matdes.2016.09.012.

[18]   Y.-Q. Zhang, G.-Z. Quan, J. Zhao, W. Xiong, Influencing Mechanisms of Prior Cold Deformation on Mixed Grain Boundary Network in the Thermal Deformation of Ni80A Superalloy, Materials (Basel). 15 (2022) 6426. https://doi.org/10.3390/ma15186426.

[19]   J. Han, S.L. Thomas, D.J. Srolovitz, Grain-boundary kinetics: A unified approach, Prog. Mater. Sci. 98 (2018) 386–476. https://doi.org/10.1016/j.pmatsci.2018.05.004.

[20]   V. Mazánová, M. Heczko, J. Polák, On the mechanism of fatigue crack initiation in high-angle grain boundaries, Int. J. Fatigue. 158 (2022) 1–7. https://doi.org/10.1016/j.ijfatigue.2022.106721.

[21]   S. Ratanaphan, D.L. Olmsted, V. V. Bulatov, E.A. Holm, A.D. Rollett, G.S. Rohrer, Grain boundary energies in body-centered cubic metals, Acta Mater. 88 (2015) 346–354. https://doi.org/10.1016/j.actamat.2015.01.069.

[22]   M. Liu, W. Gong, R. Zheng, J. Li, Z. Zhang, S. Gao, C. Ma, N. Tsuji, Achieving excellent mechanical

properties in type 316 stainless steel by tailoring grain size in homogeneously recovered or recrystallized nanostructures, Acta Mater. 226 (2022) 117629. https://doi.org/10.1016/j.actamat.2022.117629.

[23]   J. Hu, Z. Zhuang, F. Liu, X. Liu, Z. Liu, Investigation of grain boundary and orientation effects in polycrystalline metals by a dislocation-based crystal plasticity model, Comput. Mater. Sci. 159 (2019) 86–94. https://doi.org/10.1016/j.commatsci.2018.12.010.

[24]   M. Irani, M. Joun, Determination of JMAK dynamic recrystallization parameters through FEM optimization techniques, Comput. Mater. Sci. 142 (2018) 178–184. https://doi.org/10.1016/j.commatsci.2017.10.007.

[25]   S. Mandal, V. Rakesh, P. V. Sivaprasad, S. Venugopal, K. V. Kasiviswanathan, Constitutive equations to predict high temperature flow stress in a Ti-modified austenitic stainless steel, Mater. Sci. Eng. A. 500 (2009) 114–121. https://doi.org/10.1016/j.msea.2008.09.019.

[26]   R. Subbiah, V. Vinod Kumar, G. Lakshmi Prasanna, Wear analysis of treated Duplex Stainless Steel material by carburizing process - A review, Mater. Today Proc. 26 (2019) 2946–2952. https://doi.org/10.1016/j.matpr.2020.02.608.

[27]   A.M. Gatey, S.S. Hosmani, C.A. Figueroa, S.B. Arya, R.P. Singh, Role of surface mechanical attrition treatment and chemical etching on plasma nitriding behavior of AISI 304L steel, Surf. Coatings Technol. 304 (2016) 413–424. https://doi.org/10.1016/J.SURFCOAT.2016.07.020.

[28]   J.C. Dalton, F. Ernst, A.H. Heuer, Low-Temperature Nitridation of 2205 Duplex Stainless Steel, Metall. Mater. Trans. A Phys. Metall. Mater. Sci. 51 (2020) 608–617. https://doi.org/10.1007/s11661-019-05553-x.

[29]   N. Dai, J. Wu, L.C. Zhang, L. Yin, Y. Yang, Y. Jiang, J. Li, Pitting and etching behaviors occurring in duplex stainless steel 2205 in the presence of alternating voltage interference, Constr. Build. Mater. 202 (2019) 877–890. https://doi.org/10.1016/j.conbuildmat.2019.01.084.

[30]   N. Haghdadi, C. Ledermueller, H. Chen, Z. Chen, Q. Liu, X. Li, G. Rohrer, X. Liao, S. Ringer, S. Primig, Evolution of microstructure and mechanical properties in 2205 duplex stainless steels during additive manufacturing and heat treatment, Mater. Sci. Eng. A. 835 (2022) 142695. https://doi.org/10.1016/j.msea.2022.142695.

[31]   Y. Meng, S. Sugiyama, J. Yanagimoto, Effects of heat treatment on microstructure and mechanical properties of Cr-V-Mo steel processed by recrystallization and partial melting method, J. Mater. Process. Technol. 214 (2014) 87–96. https://doi.org/10.1016/j.jmatprotec.2013.08.001.

[32]   J.Y. Choi, K.T. Park, Secondary Austenite Formation During Aging of Hot-Rolled Plate of a TRIP-Aided Mo-Free Lean Duplex Stainless Steel, Met. Mater. Int. 27 (2021) 3105–3114. https://doi.org/10.1007/s12540-020-00689-7.

[33]   M.B. Mampuya, M.C. Umba, K. Mutombo, P.A. Olubambi, Effect of heat treatment on the microstructure of duplex stainless steel 2205, Mater. Today Proc. 38 (2021) 1107–1112. https://doi.org/10.1016/j.matpr.2020.06.196.

[34]   R. Ferraresi, A. Avanzini, S. Cecchel, C. Petrogalli, G. Cornacchia, Microstructural, Mechanical, and Tribological Evolution under Different Heat Treatment Conditions of Inconel 625 Alloy Fabricated by Selective Laser Melting, Adv. Eng. Mater. 24 (2022). https://doi.org/10.1002/adem.202100966.

[35]   M. Breda, K. Brunelli, F. Grazzi, A. Scherillo, I. Calliari, Effects of Cold Rolling and Strain-Induced Martensite Formation in a SAF 2205 Duplex Stainless Steel, Metall. Mater. Trans. A Phys. Metall. Mater. Sci. 46 (2015) 577–586. https://doi.org/10.1007/s11661-014-2646-x.

[36]   M. Zhao, L. Huang, C. Li, J. Li, P. Li, Evaluation of the deformation behaviors and hot workability of a high-strength low-alloy steel, Mater. Sci. Eng. A. 810 (2021) 141031. https://doi.org/10.1016/j.msea.2021.141031.

[37]   B. Liao, L. Cao, X. Wu, Y. Zou, G. Huang, P.A. Rometsch, M.J. Couper, Q. Liu, Effect of heat treatment condition on the flow behavior and recrystallization mechanisms of aluminum alloy 7055, Materials (Basel). 12 (2019). https://doi.org/10.3390/ma12020311.

[38]   Y.C. Lin, J. Huang, D.G. He, X.Y. Zhang, Q. Wu, L.H. Wang, C. Chen, K.C. Zhou, Phase transformation and dynamic recrystallization behaviors in a Ti55511 titanium alloy during hot compression, J. Alloys Compd. 795 (2019) 471–482. https://doi.org/10.1016/j.jallcom.2019.04.319.

[39]   M. Mohammadi, H.R. Ashtiani, Influence of heat treatment on the aa6061 and aa6063 aluminum alloys behavior at elevated deformation temperature, Iran. J. Mater. Sci. Eng. 18 (2021) 1–17. https://doi.org/10.22068/ijmse.1890.

[40]   H.-B. Li, M.-S. Chen, Y.-Q. Tian, L.-S. Chen, · Li, -Qing Chen, Ultra-fine-Grained Ferrite Prepared from Dynamic Reversal Austenite During Warm Deformation, 33 (2020) 290–298. https://doi.org/10.1007/s40195-019-00973-5.

[41]   Z. Li, H. Xie, F. Jia, Y. Lu, X. Yuan, S. Jiao, Z. Jiang, Study on deformation characteristics and

microstructure evolution of 2205/ah36 bimetal composite in a novel hot forming process, Metals (Basel). 10 (2020) 1–17. https://doi.org/10.3390/met10101375.

[42] E.I. Poliak, J.J. Jonas, Critical strain for dynamic recrystallization in variable strain rate hot deformation, ISIJ Int. 43 (2003) 692–700. https://doi.org/10.2355/isijinternational.43.692.

[43] R. Alturk, S. Mates, Z. Xu, F. Abu-Farha, Effects of microstructure on the strain rate sensitivity of advanced steels, Miner. Met. Mater. Ser. Part F6 (2017) 243–254. https://doi.org/10.1007/978-3-319-51493-2_24.